AMERICAN SOCIETY FOR MICROBIOLOGY | Applied and Environmental Microbiology®

ENVIRONMENTAL MICROBIOLOGY

Syntrophomonas wolfei Uses an NADH-Dependent, Ferredoxin-Independent [FeFe]-Hydrogenase To Reoxidize NADH

Nathaniel A. Losey,[a] Florence Mus,[b] John W. Peters,[b] Huynh M. Le,[a]* Michael J. McInerney[a]

Department of Plant Biology and Microbiology, University of Oklahoma, Norman, Oklahoma, USA[a]; Department of Chemistry and Biochemistry, Institute of Biological Chemistry, Washington State University, Pullman, Washington, USA[b]

ABSTRACT *Syntrophomonas wolfei* syntrophically oxidizes short-chain fatty acids (four to eight carbons in length) when grown in coculture with a hydrogen- and/or formate-using methanogen. The oxidation of 3-hydroxybutyryl-coenzyme A (CoA), formed during butyrate metabolism, results in the production of NADH. The enzyme systems involved in NADH reoxidation in *S. wolfei* are not well understood. The genome of *S. wolfei* contains a multimeric [FeFe]-hydrogenase that may be a mechanism for NADH reoxidation. The *S. wolfei* genes for the multimeric [FeFe]-hydrogenase (*hyd1ABC*; SWOL_RS05165, SWOL_RS05170, SWOL_RS05175) and [FeFe]-hydrogenase maturation proteins (SWOL_RS05180, SWOL_RS05190, SWOL_RS01625) were coexpressed in *Escherichia coli*, and the recombinant Hyd1ABC was purified and characterized. The purified recombinant Hyd1ABC was a heterotrimer with an $\alpha\beta\gamma$ configuration and a molecular mass of 115 kDa. Hyd1ABC contained 29.2 $\pm$ 1.49 mol of Fe and 0.7 mol of flavin mononucleotide (FMN) per mole enzyme. The purified, recombinant Hyd1ABC reduced NAD^+ and oxidized NADH without the presence of ferredoxin. The HydB subunit of the *S. wolfei* multimeric [FeFe]-hydrogenase lacks two iron-sulfur centers that are present in known confurcating NADH- and ferredoxin-dependent [FeFe]-hydrogenases. Hyd1ABC is a NADH-dependent hydrogenase that produces hydrogen from NADH without the need of reduced ferredoxin, which differs from confurcating [FeFe]-hydrogenases. Hyd1ABC provides a mechanism by which *S. wolfei* can reoxidize NADH produced during syntrophic butyrate oxidation when low hydrogen partial pressures are maintained by a hydrogen-consuming microorganism.

IMPORTANCE Our work provides mechanistic understanding of the obligate metabolic coupling that occurs between hydrogen-producing fatty and aromatic acid-degrading microorganisms and their hydrogen-consuming partners in the process called syntrophy (feeding together). The multimeric [FeFe]-hydrogenase used NADH without the involvement of reduced ferredoxin. The multimeric [FeFe]-hydrogenase would produce hydrogen from NADH only when hydrogen concentrations were low. Hydrogen production from NADH by *Syntrophomonas wolfei* would likely cease before any detectable amount of cell growth occurred. Thus, continual hydrogen production requires the presence of a hydrogen-consuming partner to keep hydrogen concentrations low and explains, in part, the obligate requirement that *S. wolfei* has for a hydrogen-consuming partner organism during growth on butyrate. We have successfully expressed genes encoding a multimeric [FeFe]-hydrogenase in *E. coli*, demonstrating that such an approach can be advantageous to characterize complex redox proteins from difficult-to-culture microorganisms.

KEYWORDS *Syntrophomonas*, hydrogenase, methanogenesis, syntrophs

Received 15 June 2017 **Accepted** 29 July 2017

Accepted manuscript posted online 11 August 2017

Citation Losey NA, Mus F, Peters JW, Le HM, McInerney MJ. 2017. *Syntrophomonas wolfei* uses an NADH-dependent, ferredoxin-independent [FeFe]-hydrogenase to reoxidize NADH. Appl Environ Microbiol 83:e01335-17. https://doi.org/10.1128/AEM.01335-17.

Editor Haruyuki Atomi, Kyoto University

Address correspondence to Michael J. McInerney, mcinerney@ou.edu.

* Present address: Huynh M. Le, Immuno-Mycologics, Inc. (IMMY), Norman, Oklahoma, USA.

The model syntrophic bacterium *Syntrophomonas wolfei* oxidizes butyrate to acetate with the concomitant production of hydrogen and formate (1). During syntrophic butyrate metabolism, the hydrogen- and/or formate-using methanogen maintains low levels of hydrogen and formate so that butyrate oxidation remains thermodynamically favorable (2, 3). Butyrate oxidation by *S. wolfei* involves two different oxidation-reduction reactions, generating electrons at two different redox potentials, both of which are used to produce hydrogen or formate (4–6). The first set of electrons is generated during the oxidation of butyryl-coenzyme A (butyryl-CoA) to crotonyl-CoA. Due to the high redox potential of this electron pair ($E^{o'} = -125$ mV), it has been proposed that membrane complexes utilizing chemiosmotic energy are required for hydrogen or formate production (4, 5, 7–9). The second pair of electrons is generated from the oxidation of 3-hydroxybutyryl-CoA to acetoacetyl-CoA ($E^{o'} = -250$ mV) and is used to reduce NAD^+ to NADH ($E^{o'} = -320$ mV). NADH reoxidation must be coupled to hydrogen or formate production during syntrophic butyrate metabolism. Under the low hydrogen partial pressures maintained by hydrogenotrophic methanogens (<10 Pa), the redox potential (E′) of hydrogen is about −260 mV, making hydrogen production directly from NADH thermodynamically feasible (3, 10).

The analysis of the *S. wolfei* genome identified a multimeric [FeFe]-hydrogenase encoded by genes (*hyd1ABC*; SWOL_RS05165, SWOL_RS05170, SWOL_RS05175) that shared a sequence identity similar to those of confurcating [FeFe]-hydrogenases (4, 10, 11), a NADPH-linked [FeFe]-hydrogenase (12), and NADH-dependent formate dehydrogenases (13). Most examples of multimeric [FeFe]-hydrogenases have been reported to function in either electron confurcation or the reverse (bifurcating) reaction. Confurcating [FeFe]-hydrogenases couple the unfavorable production of hydrogen from NADH with the favorable production of hydrogen from reduced ferredoxin (11), utilizing equimolar amounts of NADH and reduced ferredoxin to produce hydrogen, as was first demonstrated in the multimeric [FeFe]-hydrogenase from *Thermotoga maritima* (11). Additional multimeric [FeFe]-hydrogenases have been studied in *Acetobacterium woodii* (14), *Moorella thermoacetica* (15), and *Ruminococcus albus* (16).

The beta-oxidation of butyrate by *S. wolfei* does not directly result in the formation of reduced ferredoxin. Thus, the metabolism of *S. wolfei* differs from the metabolism of organisms with reported confurcating/bifurcating [FeFe]-hydrogenases, which have ferredoxin-dependent oxidoreductases, such as pyruvate:ferredoxin oxidoreductase, that produce reduced ferredoxin during substrate degradation (11, 14–16). One potential source of reduced ferredoxin in *S. wolfei* is a putative Fix system (nitrogen fixation), which could produce reduced ferredoxin from the oxidation of NADH (4). However, the use of Fix to produce reduced ferredoxin would place a high energy demand on an organism that uses growth reactions that operate close to thermodynamic equilibrium (17). In the absence of an identifiable source of reduced ferredoxin and with syntrophic growth conditions that would be permissive for hydrogen production from NADH, it is likely that Hyd1ABC functions as a nonconfurcating, NADH-dependent [FeFe]-hydrogenase.

We cloned and expressed the genes of a multimeric [FeFe]-hydrogenase (SWOL_RS05165, SWOL_RS05170, SWOL_RS05175) from *S. wolfei* and characterized the recombinant protein in order to understand the mechanisms by which *S. wolfei* reoxidizes NADH. To obtain an active enzyme, it was also necessary to coexpress the genes required for [FeFe]-hydrogenase maturation (SWOL_RS05180, SWOL_RS05190, SWOL_RS01625). This strategy has been used successfully in the past to produce active [FeFe]-hydrogenases using *Escherichia coli* (18, 19) and allowed the production of an enzyme with the activity of a NADH-dependent [FeFe]-hydrogenase (Hyd1ABC: SWOL_RS05165, SWOL_RS05170, SWOL_RS05175 gene products).

RESULTS

Purification and molecular weight. The recombinant gene products of SWOL_RS05165, SWOL_RS05170, and SWOL_RS05175 were purified to apparent homogeneity using nickel affinity and anion exchange chromatography, resulting in an apparent

TABLE 1 Purification of the NADH-dependent [FeFe]-hydrogenase Hyd1ABC

Fraction	Protein (mg)	Activity $H_2 \rightarrow MV_{ox}$ ($U \cdot mg^{-1}$)[a]		Purification (fold)	Yield (%)
		Specific	Total		
Cell extract	670	16.8	11,200	1	100
HisTrap HP	4.0	655	2,620	38.9	23.4
UNO-Q1	0.43	3,340	1,430	199	12.7

[a]Activity was determined at 37°C, pH 7.5; 1 unit of activity (U) equals 2 μmol of electrons transferred per minute. MV_{ox}, oxidized methyl viologen.

yield of 12.7% (Table 1). Approximately 0.55 mg of purified recombinant enzyme was obtained from 10.8 g (wet weight) of cells. Sodium dodecyl sulfate-polyacrylamide gel electrophoresis (SDS-PAGE) analysis showed that the purified recombinant enzyme consisted of three subunits with molecular weights that were consistent with molecular weights predicted from the sequence of encoding genes, namely, 63 kDa compared to the predicted 63.0 kDa (HydA1), 43 kDa compared to the predicted 43.9 kDa (HydB1), and 13 kDa compared to the predicted 17.5 kDa (HydC1) with the included molecular weight of the His tag (MGSSHHHHHHSQDP, 1.6 kDa) (Fig. 1). Native PAGE analysis showed that the purified enzyme migrated as a single band (Fig. 2), and size exclusion chromatography gave a molecular mass of 115 kDa. The single visible band from native gel electrophoresis when subjected to peptide analysis showed high coverage scores for the intended peptides (Table S1). Based on the subunit analysis and the native molecular weight, Hyd1ABC is a heterotrimer with an $\alpha\beta\gamma$ configuration and a molecular mass of 124.5 kDa as predicted by the sequence of the encoding genes. Iron content was determined to be 29.2 $\pm$ 1.49 mol of Fe per mole of enzyme, which matches well with the predicted 30 mol Fe per mole of enzyme from conserved domain analysis, which indicated five [4Fe-4S] clusters, two [2Fe-2S] clusters, and the six Fe in the [H] cluster. The flavin content was 0.7 mol of flavin mononucleotide (FMN) per mole of enzyme, which agrees with the single flavin-binding site in the HydB subunit, predicted from conserved domain analysis.

Activity. The purified recombinant Hyd1ABC had high hydrogen-dependent methyl viologen-reducing activity and reduced methyl viologen-oxidizing activity (Table 2), typical for many [FeFe]-hydrogenases. The purified recombinant Hyd1ABC also had high NAD^+-reducing activity with hydrogen as the electron donor (specific activity of

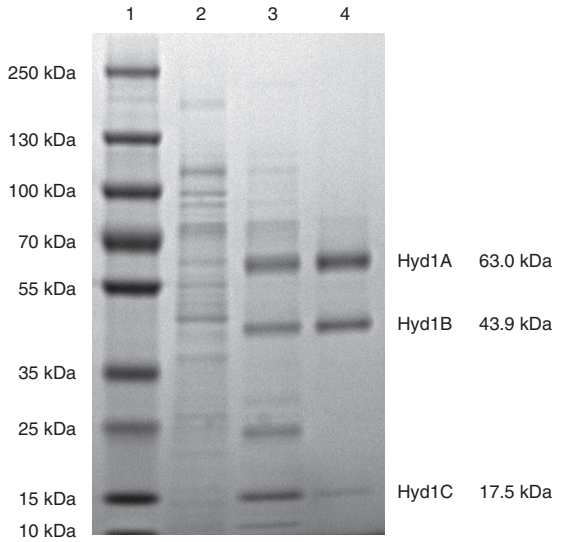

FIG 1 SDS-PAGE of the NADH-dependent [FeFe]-hydrogenase Hyd1ABC. Lanes: 1, molecular mass markers; 2, *E. coli* cell extract; 3, HisTrap HP; 4, UNO-Q1. The displayed molecular masses of Hyd1A-C peptides are predicted from the amino acid sequence.

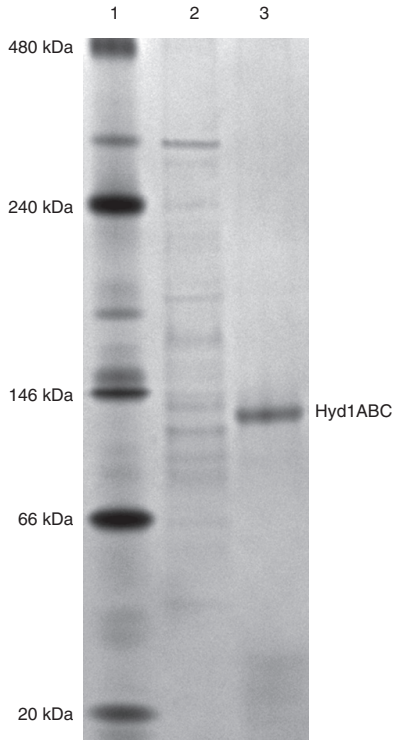

FIG 2 Native PAGE of the NADH-dependent [FeFe]-hydrogenase Hyd1ABC. Lanes: 1, native molecular mass markers; 2, *E. coli* cell extract; 3, UNO-Q1 fraction of the purified Hyd1ABC.

94.5 U · mg^{-1} at 37°C) and catalyzed hydrogen production from NADH with a specific activity of 6.6 U · mg^{-1} at 37°C (Table 2). The enzyme neither oxidized NADPH nor reduced $NADP^+$ under any condition tested. Neither the rate of NAD^+ reduction nor the rate of NADH-dependent hydrogen production changed when oxidized or reduced clostridial ferredoxin, respectively, was added (Fig. 3 and 4). In addition, the purified recombinant Hyd1ABC did not reduce clostridial ferredoxin either alone or in the presence of NAD^+ with hydrogen as the electron donor. Hyd1ABC did not produce hydrogen from reduced clostridial ferredoxin in the absence of NADH, and the amount of hydrogen produced when both NADH and reduced ferredoxin were present was similar to that produced when only NADH was present (Fig. 4). The above-described

TABLE 2 Specific activities of the purified NADH-dependent [FeFe]-hydrogenase Hyd1ABC

Reaction[a]	Hydrogenase activity (U · mg^{-1})[b]
$H_2 \rightarrow MV_{ox}$	571
$H_2 \rightarrow NAD^+$	94.5
$H_2 \rightarrow NAD^+ + Fd_{ox}$	92.1[c]
$H_2 \rightarrow NADP^+$	<0.01
$H_2 \rightarrow NADP^+ + Fd_{ox}$	<0.01
$H_2 \rightarrow Fd_{ox}$	<0.01
$MV_{red} \rightarrow H_2$	24.3
$NADH \rightarrow H_2$	6.6
$NADH + Fd_{red} \rightarrow H_2$	6.0
$NADPH \rightarrow H_2$	<0.01
$NADPH + Fd_{red} \rightarrow H_2$	<0.01
$Fd_{red} \rightarrow H_2$	<0.01

[a]MV_{ox}, oxidized methyl viologen; FD_{ox}, oxidized ferredoxin; MV_{red}, reduced methyl viologen; FD_{red}, reduced ferredoxin.

[b]Activity was determined at 37°C, pH 7.5; 1 unit of activity (U) equals 2 μmol of electrons transferred per minute.

[c]Activity is the rate of NAD^+ reduction at 340 nm in the presence of Fd_{ox} and not the rate of Fd_{ox} reduction (at 430 nm), which was not observed to occur.

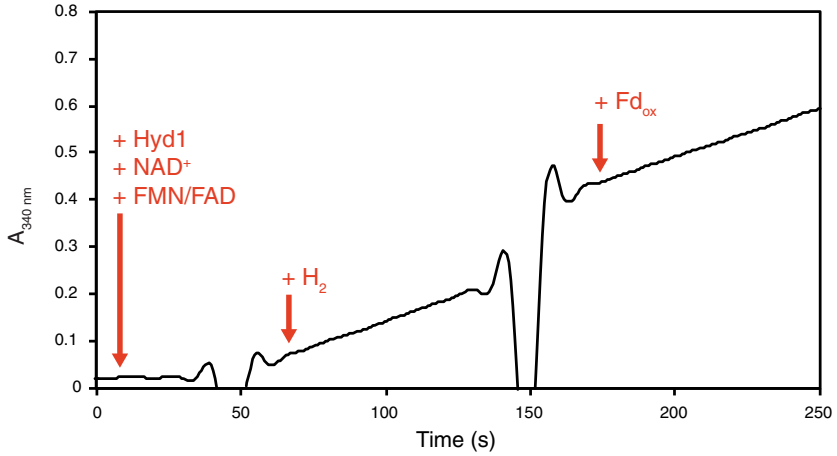

FIG 3 Reduction of NAD^+ by the purified, NADH-dependent [FeFe]-hydrogenase Hyd1ABC with hydrogen as the electron donor. Reactions were performed in 1.5-ml, sealed, anaerobic cuvettes containing 0.5 ml of 50 mM potassium phosphate buffer (pH 7.5 at 37°C), 5 μM FAD, 5 μM FMN, 2 mM DTE, 1 mm NAD^+, and 0.11 μg of Hyd1ABC. Clostridial ferredoxin (Fd_{ox}) was added at a concentration of 10 μM. The change in absorbance (ΔA_{340}) before the addition of hydrogen was 0.129 A · min^{-1}, and after the addition of oxidized ferredoxin it was 0.125 A · min^{-1}.

experiments were repeated with the purified recombinant *S. wolfei* ferredoxin encoded by SWOL_RS10890 with results similar to those using the clostridial ferredoxin. That is, the recombinant *S. wolfei* ferredoxin did not appear to affect the rate of NAD^+ reduction or NADH oxidation. In addition, Hyd1ABC did not reduce the recombinant *S. wolfei* ferredoxin with hydrogen as the electron donor and did not produce hydrogen with reduced recombinant *S. wolfei* ferredoxin as the electron donor. The kinetics of NAD^+ reduction with hydrogen, where the NAD^+ concentration was varied, indicated a K_m for NAD^+ of 520 μM, a V_{max} of 196 U · mg^{-1}, and a k_{cat} of 406.7 s^{-1}, assuming a single catalytic site per a molecular mass of 124.5 kDa (see Fig. S1 in the supplemental material). Hyd1ABC specific activities for methyl viologen and NAD^+ reduction and for NADH oxidation were similar to those reported for other multimeric [FeFe]-hydroge-

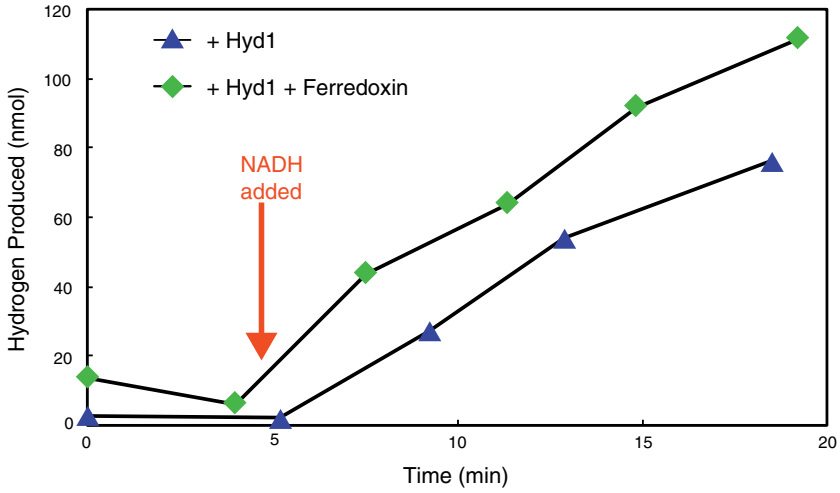

FIG 4 The effect of NADH and reduced ferredoxin on hydrogen production by Hyd1ABC. Reactions were performed in 6.5-ml serum bottles containing 0.5 ml of 100 mM potassium phosphate buffer (pH 7.5 at 37°C), 5 μM FAD, 5 μM FMN, 2 mM DTE, 1 mM NADH, and 1.3 μg of Hyd1ABC. A ferredoxin reduction system as indicated by "+ Ferredoxin" consisted of 10 mM pyruvate, 1 mM CoA, 0.1 mM thiamine pyrophosphate, 5 μM clostridial ferredoxin, and 0.1 U of clostridial pyruvate:ferredoxin oxidoreductase. NADH (1 mM) was added immediately after sampling time points indicated by the red arrow.

TABLE 3 Equilibrium hydrogen partial pressures produced by the NADH-dependent [FeFe]-hydrogenase Hyd1ABC at different pH values and NADH/NAD^+ ratios[a]

Condition	NADH/NAD^+ ratio	Mean (range) hydrogen partial pressure (Pa)	Hydrogen produced (nmol)
pH 6.5, 2.0 mM NAD^+, 3.0 mM NADH	1.5	40.0 (6.9)	95.4
pH 6.5, 2.5 mM NAD^+, 2.5 mM NADH	1.0	21.8 (8.7)	51.8
pH 7.0, 2.0 mM NAD^+, 3.0 mM NADH	1.5	25.9 (0.8)	61.9
pH 7.0, 2.5 mM NAD^+, 2.5 mM NADH	1.0	17.0 (11.3)	40.4

[a]Assays were performed in 6.5-ml serum bottles with 0.5 ml of liquid volume containing 0.86 μg of protein and 6 ml of headspace.

nases; however, the K_m for reduction of NAD^+ by Hyd1ABC was higher than that of other multimeric [FeFe]-hydrogenases (Table S2).

In the above-described assays, the purified Hyd1ABC produced hydrogen from NADH under conditions where only a small amount of NADH would be oxidized to NAD^+ during the time course of the assay and thus the ratio of NADH to NAD^+ would remain high. To determine whether Hyd1ABC could produce hydrogen from NADH under more physiological conditions, we varied the ratio of NADH to NAD^+ and the pH but kept the total pyridine nucleotide concentration constant at 5 mM (Table 3). In each case, more hydrogen was produced with a NADH/NAD^+ ratio of 1.5 than with a ratio of 1.0. More hydrogen was also produced at pH 6.5 than at pH 7.0. Hydrogen partial pressures varied from 17.0 Pa, with a range of 11.3 Pa, to 40.0 Pa with a range of 6.9 Pa, with higher partial pressures observed at lower pH values and higher NADH/NAD^+ ratios. Final hydrogen partial pressures detected in these experiments were below those predicted at thermodynamic equilibrium for the given NADH/NAD^+ ratios. With the given liquid and gas volumes, a NADH/NAD^+ ratio of 1.5, and a pH of 7.0, the redox potential (E′) of the NADH/NAD^+ pair should be greater than −320 mV, even with the shift in NADH/NAD^+ ratio as NADH is oxidized. The predicted equilibrium hydrogen partial pressure is in excess of 70 Pa for these conditions; however, the measured hydrogen partial pressure was lower, at 25.9 Pa, with a range of 0.8, suggesting that thermodynamic equilibrium was not reached.

Hydrogen levels in growing coculture. Hydrogen partial pressures measured during growth of *S. wolfei* in coculture with *Methanospirillum hungatei* on either butyrate or crotonate were between 4.6 and 18.0 Pa (Fig. S2), with the highest concentrations observed at day four and lower concentrations observed during the later stages of growth. Hydrogen partial pressures measured for pure culture *S. wolfei* grown on crotonate were between 27.4 and 40.0 Pa.

DISCUSSION

The identification of a NADH-dependent [FeFe]-hydrogenase in *S. wolfei* provides an explanation for how electrons derived from 3-hydroxybutyryl-CoA oxidation are used to make hydrogen during syntrophic growth. Stoichiometrically, all electrons derived from the oxidation of butyrate are converted to either hydrogen or formate, as *S. wolfei* does not produce any other reduced end products during syntrophic butyrate metabolism (20, 21). The electrons generated by the oxidation of 3-hydroxybutyryl-CoA to acetoacetyl-CoA are used to reduce NAD^+ to NADH (6). The presence of genes encoding a multimeric [FeFe]-hydrogenase and NADH-linked formate dehydrogenase in the genome of *S. wolfei* (4) suggested that NADH could be reoxidized using these enzyme systems. Hyd1 represents the only hydrogenase encoded within the genome of *S. wolfei* predicted to catalyze NADH oxidation. Of the two other hydrogenases present within the *S. wolfei* genome, Hyd2, encoded by SWOL_RS09950, is a membrane-bound [FeFe]-hydrogenase believed to interact with the menaquinone pool (4, 7, 8), while Hyd3, encoded by SWOL_RS12620, is a monomeric type [FeFe]-hydrogenase (4), which has not been reported to interact with NADH (22). The *hyd1A* gene was upregulated under coculture conditions on butyrate compared to coculture conditions on crotonate (9), and Hyd1ABC was confirmed to be present by proteomic techniques (5, 7) during syntrophic coculture growth on butyrate with *M. hungatei*.

Thus, Hyd1ABC along with NADH-linked formate dehydrogenases are the likely routes of NADH reoxidation in *S. wolfei*.

The possibility that *S. wolfei* utilizes a NADH-dependent hydrogenase was suggested previously due to the closeness of the redox potentials of 3-hydroxybutyryl-CoA/acetoacetyl-CoA ($E^{o'} = -250$ mV), NADH/NAD^+ ($E^{o'} = -320$ mV), and H_2/H^+ at 1 Pa H_2 ($E' = -261$ mV) (3). The amino acid sequence comparisons suggested that Hyd1ABC might be a confurcating hydrogenase (4, 10). Confurcating/bifurcating [FeFe]-hydrogenses produce hydrogen from NADH ($E^{o'} = -320$ mV) and reduced ferredoxin ($E^{o'} = -398$ mV or less) (11, 23). Coupling the unfavorable hydrogen production from NADH with the favorable hydrogen production from reduced ferredoxin would allow hydrogen production at partial pressures greater than 1,000 Pa at equilibrium (equivalent to $E' = -367$ mV). The NADH/NAD^+ midpoint potential ($E^{o'} = -320$ mV) would allow for a much lower hydrogen partial pressure of close to 70 Pa at equilibrium. Using fixed NADH/NAD^+ ratios of 1.0 and 1.5, Hyd1ABC produced partial pressures of hydrogen of 17 to 40 Pa (Table 3). NADH/NAD^+ ratios reported for organisms grown under anaerobic conditions can vary, with some values lower than those tested here, for example, 0.27 for *Clostridium kluyveri*, 0.29 for *Clostridium welchii*, and 0.4 for *E. coli* (24), while other studies have reported higher ratios of 0.75 for *E. coli* (25) and 1.16 for *Enterococcus faecalis* (26). Thus, the production of hydrogen by Hyd1ABC from NADH/NAD^+ ratios of 1.0 or higher resembles physiological conditions for *S. wolfei* cells, although the actual NADH/NAD^+ ratios during syntrophic growth conditions have not yet been determined.

The partial pressure of hydrogen produced by Hyd1ABC was within the range of the hydrogen partial pressure (25 Pa) produced by suspensions of butyrate-grown *S. wolfei* cells when conditions allowed only hydrogen production from NADH (27). Butyrate-oxidizing cocultures of *S. wolfei* and *Methanobacterium formicicum* maintained a partial pressure of hydrogen of 10.6 Pa (28), while hydrogen concentrations for cocultures of *S. wolfei* and *M. hungatei* ranged from 4.6 to 18.0 Pa (Fig. S2). Measurements of partial pressures of hydrogen from methanogenic butyrate-degrading environments, such as lake sediment and sewage sludge, ranged from 3.7 to 26.9 Pa (29). Hydrogen partial pressures from syntrophic, butyrate-oxidizing biogas reactors ranged from 1 to 4.5 Pa (30). Methanogenic syntrophic microcosms established from peat soil implicated members of the *Syntrophomonas* genus in butyrate oxidation and had hydrogen partial pressures that ranged from 3 to 12.5 Pa (31). Thus, the hydrogen partial pressure that would allow for reoxidation of NADH during syntrophic butyrate metabolism is considerably less than that achieved by confurcating hydrogenases, but it is within the range of the hydrogen partial pressures produced by Hyd1ABC from NADH alone (Table 3). Furthermore, such hydrogen partial pressures are observed in coculture, microcosms, and environments where members of the *Syntrophomonas* genus would perform syntrophic butyrate oxidation. Thus, the hydrogen partial pressure achieved by Hyd1ABC from NADH would appear to be sufficient to allow syntrophic growth of *S. wolfei* on butyrate in coculture with a hydrogenotrophic methanogen.

Hyd1ABC was capable of both the reduction of NAD^+ with hydrogen and the oxidation of NADH to produce hydrogen in the absence of ferredoxin (Fig. 3 and 4; Table 2), indicating the lack of the tight coupling that is reported for bifurcating/confurcating [FeFe]-hydrogenases (11, 14, 15). In addition, Hyd1ABC did not reduce ferredoxin even in the presence of NAD^+. Thus, if Hyd1ABC is capable of producing hydrogen using electrons from reduced ferredoxin under as-yet-unidentified conditions, the concomitant reduction of NAD^+ by hydrogen would result in hydrogen being equilibrated with the redox potential of the NADH/NAD^+ pool, preventing higher hydrogen partial pressures that would normally be achievable by confurcating hydrogenases. It is not surprising that Hyd1 does not interact with ferredoxin. Ferredoxin levels are very low in the proteome of *S. wolfei* (7), and we did not detect ferredoxin using the traditional approach to purify ferredoxin (N. Losey and M. J. McInerney, unpublished data), e.g., elution from an ion exchange column after high salt treatment and monitoring of the $A_{390}/_{280}$ ratio (32, 33). Unlike other organisms known to possess

confurcating hydrogenases (11, 14–16), *S. wolfei* does not have a clear mechanism or need to produce reduced ferredoxin in amounts equivalent to the amount of NADH made from butyrate (4, 5). Microorganisms known to possess confurcating [FeFe]-hydrogenases, such as *T. maritima* (11), *M. thermoacetica* (15), and *R. albus* (16), have fermentative metabolisms with ferredoxin-dependent enzymes such as pyruvate:ferredoxin oxidoreductase, which can produce reduced ferredoxin in amounts needed for the coupled hydrogen production from NADH. However, *S. wolfei* uses fatty acids exclusively as the substrates for growth (1, 21, 34). Beta-oxidation of fatty acids by *S. wolfei* results in the formation of reduced electron transfer flavoprotein and NADH but not directly in reduced ferredoxin (6).

The presence of both HydB/HydC subunits has been suggested as being more determining for identifying bifurcating [FeFe]-hydrogenases than the composition of the HydA subunit (22). Compared to the iron-sulfur centers of known bifurcating/confurcating [FeFe]-hydrogenases, the iron-sulfur centers of *S. wolfei* Hyd1ABC have two differences as predicted by NCBI's Conserved Domain Database (35) that may relate to its inability to use ferredoxin as an electron donor (Fig. 5). The HydB1 subunit lacks an N-terminal [2Fe-2S] cluster and a C-terminal [4Fe-4S] cluster. The difference is reflected in the overall peptide length of *S. wolfei* HydB1 of 407 amino acid residues compared to the approximately 600 residues for HydB subunits of known bifurcating [FeFe]-hydrogenases. The reportedly nonconfurcating, NADPH-dependent [FeFe]-hydrogenase from *Desulfovibrio fructosivorans* also lacks an N-terminal [2Fe-2S] cluster in its HydB subunit (Fig. 5) (12). The number of iron-sulfur centers also seems to match with the ability to bifurcate in multimeric molybdopterin formate dehydrogenases. The multimeric, molybdopterin formate dehydrogenase from *Clostridium acidurici* has been shown to catalyze electron bifurcation and has the same iron-sulfur centers in its HydB and HydC equivalent subunits that known bifurcating [FeFe]-hydrogenases have while a nonbifurcating, NADH-dependent formate dehydrogenase from *Rhodobacter capsulatus* lacks a C-terminal [4Fe-4S] cluster in its HydB subunit (13, 36). The NADH-dependent [FeFe]-hydrogenase from *Caldanaerobacter* (formerly *Thermoanaerobacter*) *tengcongensis* may be an example of an enzyme whose number of iron-sulfur centers is equivalent to those of bifurcating [FeFe]-hydrogenases but with the ability to reduce NAD^+ and oxidize NADH without ferredoxin (37). However, the *C. tengcongensis* [FeFe]-hydrogenase was not tested under bifurcating/confurcating conditions by supplying ferredoxin in the presence of NAD^+ or NADH. While the number of examples of known bifurcating/confurcating and nonbifurcating [FeFe]-hydrogenases and formate dehydrogenases is small, it appears that the type and number of conserved iron-sulfur domains in the HydB/HydC subunits may be important for electron bifurcation activity. Electron bifurcation involves two independent paths of electron flow, either away from the bifurcation site for bifurcating enzymes or toward the bifurcation site for confurcating enzymes (38, 39). A change in the presence of an iron-sulfur cluster or its ability to facilitate the directionality of electron flow due to a change in redox potential or its distance from other redox centers may affect the bifurcation reaction. It is also possible that the loss of the ability to bifurcate was independent of the change in the number of iron-sulfur clusters and such centers were eliminated over time as they no longer served a critical function.

Multimeric [FeFe]-hydrogenases with the same number of iron-sulfur centers as *S. wolfei* Hyd1ABC are present in the genomes of other members of the family *Syntrophomonadaceae* (see Table S3 in the supplemental material). This suggests that *Syntrophomonas zehnderi*, *Syntrophothermus lipocalidus*, and *Thermosyntropha lipolytica*, which perform syntrophic oxidation of fatty acids in coculture with hydrogenotrophic methanogens (40–42), may also utilize nonconfurcating, NADH-dependent hydrogen production. Future studies of additional multimeric [FeFe]-hydrogenases may allow the determination of the relationship, if any, between certain iron-sulfur centers in the HydB and HydC subunits and the ability to perform electron bifurcation.

The [FeFe]-hydrogenase in *Syntrophobacter fumaroxidans* lacks a C-terminal [4Fe-4S] domain in the HydB subunit, which differs from reported bifurcating [FeFe]-

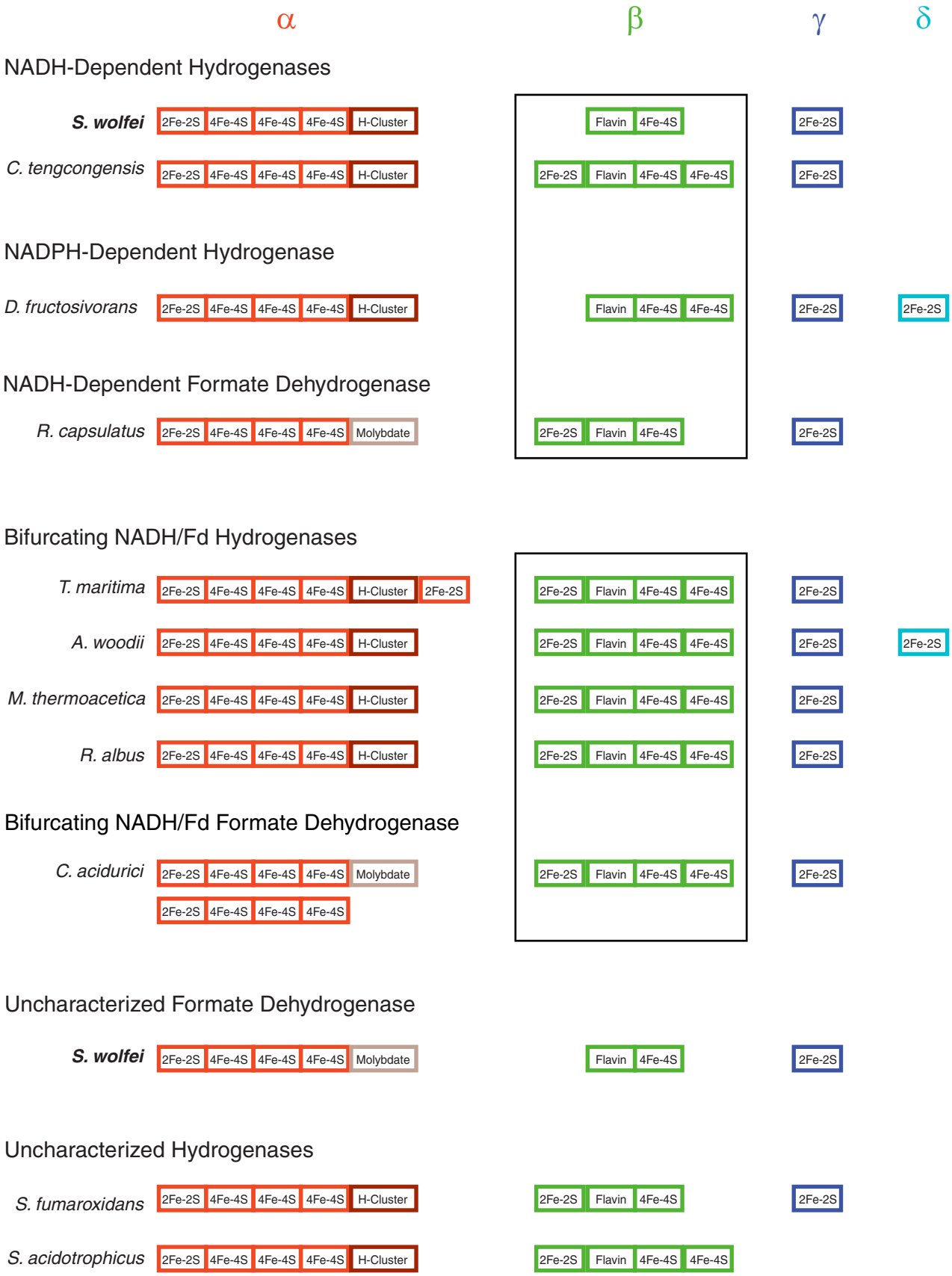

FIG 5 Comparison of predicted conserved domains present in characterized multimeric [FeFe]-hydrogenases and multimeric formate dehydrogenases.

(Continued on next page)

hydrogenases (Fig. 5). However, the metabolism of propionate by the methylmalonyl-CoA pathway by *S. fumaroxidans* leads to pyruvate formation and the ability to produce reduced ferredoxin, which is required as the low potential donor for electron bifurcation (43). The [FeFe]-hydrogenase in *Syntrophus aciditrophicus* lacks the HydC subunit, which contains a [2Fe-2S] domain (Fig. 5). *S. aciditrophicus* may also have the ability to generate reduced ferredoxin if the acyl-CoA dehydrogenases involved in cyclohex-1-ene-1-carboxylate and cyclohexane-1-carboxylate formation can catalyze electron bifurcation (44). The syntrophic metabolism of ethanol and lactate are believed to generate reduced ferredoxin (3, 10, 45). The partial pressures observed during syntrophic ethanol oxidation by cocultures of *Pelobacter* species with *M. hungatei* exceeded 1,000 Pa (46), which would not be thermodynamically favorable if NADH was the only electron donor for hydrogen production. Given the higher hydrogen partial pressures and presence of reduced ferredoxin-generating systems, it seems likely that some syntrophic oxidizers may utilize ferredoxin, possibly in a confurcating mechanism, for hydrogen production.

The *S. wolfei* Hyd1ABC was previously found to copurify with a multimeric formate dehydrogenase encoded by SWOL_RS03955, SWOL_RS03960, SWOL_RS03965, and SWOL_RS03970 (47). The copurification of Hyd1ABC with an apparent formate dehydrogenase suggested a possible formate dehydrogenase-hydrogenase complex, although an alternative would be that Hyd1 and the multimeric formate dehydrogenase are separate complexes that copurify, perhaps due to the similar nature of the HydB/HydC subunits (Fig. 5). Either as separate complexes or as a single larger complex, Hyd1 and the multimeric formate dehydrogenase could function to convert NADH to hydrogen and formate, respectively, which would mean that both metabolites are linked to the NADH/NAD^+ pool.

The identification of Hyd1ABC as a NADH-dependent hydrogenase suggests that NADH-dependent hydrogen production occurs during syntrophic growth on butyrate by *S. wolfei* without the need for reduced ferredoxin. Ferredoxin-independent hydrogen production from NADH would allow *S. wolfei* to avoid the energetically costly reaction to produce reduced ferredoxin from NADH. Based on the hydrogen partial pressures generated by Hyd1ABC (Table 3), continual NADH-dependent hydrogen production would require the presence of a hydrogen-consuming organism to maintain a low hydrogen partial pressure. NADH-dependent hydrogen production could explain in part the obligate requirement *S. wolfei* has for a hydrogen-consuming organism such as *M. hungatei* during growth on energetically poor substrates such as butyrate.

MATERIALS AND METHODS

Plasmids and strains. Genes encoding a putative multimeric [FeFe]-hydrogenase were amplified by PCR from *S. wolfei* genomic DNA with Phusion High-Fidelity DNA polymerase (Thermo Fisher Scientific, Waltham, MA) using the primers listed in Table 4. An amplicon with genes encoding HydA, HydB, and HydC (SWOL_RS05165, SWOL_RS05170, SWOL_RS05175) with the addition of BamHI and AscI restriction sites was inserted into the first multiple cloning site (MCS) of pETDuet-1 (Novagen, Merck KGaA, Darmstadt, Germany) (see Fig. S3 in the supplemental material) with the addition of an N-terminal $(His)_6$ residue on HydC to produce pETDuet-1 SwHydABC.

A second plasmid was created to express genes encoding [FeFe]-hydrogenase maturation proteins. The Hyd maturases HydE (SWOL_RS05180) and HydG (SWOL_RS05190), as well as a 348-bp open reading frame with no identifiable conserved domains (SWOL_RS05185), were amplified from the *S. wolfei* genomic template with the addition of NcoI and BamHI restriction sites and were inserted into the MCS of pCDFDuet-1 (Novagen, Merck KGaA, Darmstadt, Germany) (Fig. S1). In addition, the gene encoding the

FIG 5 Legend (Continued)
The boxes highlight the heterogeneity in the number of conserved domains in HydB (β) subunits of characterized nonbifurcating NADH-dependent [FeFe]-hydrogensases and formate dehydrogenases compared to the similarity of conserved domains of the HydB (β) subunits of characterized bifurcating [FeFe]-hydrogenases and a bifurcating formate dehydrogenase. Heterogeneity in conserved domains is also present in two unstudied [FeFe]-hydrogenases from syntrophic metabolizers *S. aciditrophicus* and *S. fumaroxidans* and a formate dehydrogenase from *S. wolfei* previously found to copurify with Hyd1ABC. The figure is a visual representation of the conserved domains as predicted by NCBI's Conserved Domain Database (40). Greek symbols at the top are the subunit designations. Accession numbers for the sequences of the subunits are given in Table S3. Reported functions of enzymes were obtained from the following references: *S. wolfei* hydrogenase (this publication), *C. tengcongensis* (37), *D. fructosivorans* (12), *R. capsulatus* (13), *T. maritima* (11), *A. woodii* (14), *M. thermoacetica* (15), *R. albus* (16), and *C. acidurici* (36).

TABLE 4 List of primers used for construction of pETDuet-1 SwHydABC, pCDFDuet-1 SwHydEFG, and pCDFDuet-1 SwFd

Primers (F, R)[a]	Function
CGCGGATCCGATGATGGATTATAAGGAGATAATTGCCCAG, TTGGCGCGCCCTATAAGAATTTTTTATTCTTGGCATGG	Amplify SWOL_RS05165, SWOL_RS05170, SWOL_RS05175, addition of restriction cut sites for BamHI/AscI
TAACCATATGCAGGATACTCCCAAAGCTA, TAACCTCGAGTTAAAGAATTGCTCGGACCCTG	Amplify SWOL_RS01625, addition of restriction cut sites for NdeI/XhoI
TTCACCATGGAAGCGATATCAGTTAACC, ACATGGATCCTTAAACCTGCTTCAAAGG	Amplify SWOL_RS05180, SWOL_RS05185, SWOL_RS05190, addition of restriction cut sites for NcoI/BamHI
CTTAGGATCCGATGTCTTACATCATC, AGTGATAAGCTTTTAGTCGTCCG	Amplify SWOL_RS010890, addition of restriction cut sites for BamHI/HindIII

[a]Underlined regions indicate restriction enzyme cut sites. F, forward; R, reverse.

Hyd maturase HydF (SWOL_RS01625) was amplified with restriction sites for NdeI and XhoI and inserted into the second MCS of pCDFDuet-1 to generate pCDFDuet-1 SwHydEFG.

In addition, a gene encoding a putative ferredoxin, SWOL_RS010890, was amplified by PCR with the addition of BamHI and HindIII restriction sites and inserted into the first MCS of pCDFDuet-1 with the addition of an N-terminal $(His)_6$ residue to generate pCDFDuet-1 SwFd. SWOL_RS010890 is predicted to encode a 6-kDa peptide containing a conserved domain for two [4Fe-4S] centers. The SWOL_RS010890 gene product shares 57% amino acid sequence identity with the ferredoxin from *Clostridium pasteurianum* (GenBank accession number M11214).

Due to changes in the locus tags for *S. wolfei* genes, a table listing the newly assigned locus tags for *S. wolfei* used in this publication, older *S. wolfei* locus tags, and GenBank protein accession numbers is included as Table S4. *S. wolfei* gene sequences included in this article are available from the *S. wolfei* genome (GenBank accession number NC_008346), which was published previously (4).

Expression conditions. *E. coli* BL21(DE3) (Thermo Fisher Scientific, Waltham, MA) cells for expression of the genes for His-tagged hydrogenase and His-tagged ferredoxin were grown in LB medium with 50 mM potassium phosphate (pH 7.5) and 10 g · liter^{-1} glucose with appropriate antibiotics at 37°C. Cultures were grown aerobically with shaking at 200 rpm to an optical density $(OD)_{600}$ of 0.4 to 0.6 before induction by the addition of 0.5 mM IPTG (isopropyl-β-D-thiogalactopyranoside), followed by the addition of 2 mM ferric ammonium citrate, 10 mM sodium fumarate, and 2 mM cysteine. After induction, the cultures were sealed with rubber stoppers and sparged with nitrogen gas for 6 h until harvesting. Cells were harvested anaerobically by centrifugation at 6,000 × *g* for 20 min at 4°C, washed by resuspension in 50 mM potassium phosphate (pH 7.5) and then pelleted again by centrifuging at 6,000 × *g* for 10 min at 4°C. The final cell pellets were frozen in liquid N_2 until further use.

Purification of His-tagged NADH-dependent hydrogenase. All manipulations, including cell harvesting and protein purification, were performed inside a Coy chamber with an atmosphere of 95% nitrogen and 1 to 5% hydrogen. All purification buffers were prepared anoxically and contained 2 mM dithioerythritol (DTE) and 5 μM both flavin adenine dinucleotide (FAD) and FMN. Cell pellets (10.8 g) were thawed and suspended in 20 ml of 50 mM Tris-HCl (pH 7.5) with 0.5 M NaCl and 30 mM imidazole, and the cells broken by passage through a French pressure cell operating at an internal pressure of 140 megapascals (MPa). Cell debris was removed by centrifugation at 13,000 × *g* for 20 min at 4°C and passage through a 0.22-μm filter. Resulting cell lysate was applied to a HisTrap HP 5-ml column (GE Healthcare Life Sciences, Pittsburgh, PA) equilibrated with the buffer used for cell breakage, followed by a wash with 50 mM imidazole in the breakage buffer, and His-tagged, NADH-dependent hydrogenase was eluted with 250 mM imidazole in the breakage buffer. Eluted fractions were then concentrated and desalted using an Amicon Ultra 0.5-ml centrifugal filter (EMD Millipore) with a 100-kDa nominal molecular mass limit filter. The desalted fractions were applied to a UNO-Q1 (Bio-Rad, Hercules, CA) column equilibrated with 50 mM Tris-HCl (pH 7.5) and eluted with a gradient of 0 to 0.6 M NaCl over a 17-min period at a flow rate of 2 ml/min. The purified protein was then aliquoted into several vials and flash frozen in liquid nitrogen until used for further analyses.

His-tagged *S. wolfei* ferredoxin was prepared as described for the His-tagged NADH-dependent hydrogenase, but the purification procedure ended after the HisTrap HP chromatography step.

Enzymatic assays. All assays were performed at 37°C unless noted otherwise. Enzyme activity measurements were determined in triplicate with various concentrations of protein to ensure activity was proportional to the amount of protein added. Hydrogenase-oxidizing activity was measured in rubber stopper-sealed, 1.4-ml quartz cuvettes (Nova Biotech, El Cajon, CA) with 600 μl of reaction mix and with hydrogen at a pressure of $1.2 \cdot 10^5$ Pa. The reaction mixture for hydrogen-oxidizing assays consisted of 50 mM Tris-HCl (pH 7.5) or potassium phosphate (pH 7.5), 2 mM DTE, 5 μM FAD, and 5 μM FMN. $NAD(P)^+$ reduction was tested with 1 mM $NAD(P)^+$ with and without 10 μM *C. pasteurianum* ferredoxin. Methyl viologen reduction assays were performed using a concentration of 10 mM methyl viologen. Reactions were initiated by either the addition of enzyme or by the addition of $1.2 \cdot 10^5$ Pa of hydrogen to a 100% nitrogen headspace. The kinetic constants for NAD^+ reduction by hydrogen were determined with various NAD^+ concentrations (0 to 2.0 mM). Spectrophotometric measurements for the reduction of NAD^+ and $NADP^+$ were performed at 340 nm (ε = 6.2 mM^{-1} cm^{-1}). Clostridial ferredoxin reduction was measured at 430 nm ($\varepsilon_{\Delta ox\text{-}red} \approx$ 13.1 mM^{-1} cm^{-1}) and methyl viologen reduction at 600 nm (ε = 10.0 mM^{-1} cm^{-1}).

Hydrogen-producing activities were measured in serum bottles (6.5 ml) sealed with butyl rubber stoppers with a 0.5-ml reaction mixture and shaking at 200 rpm. The reaction mix consisted of 100 mM

potassium phosphate at pH 7.5, unless otherwise indicated, as well as 2 mM DTE, 5 μM FAD, and 5 μM FMN. Reactions for hydrogen production were initiated by either the addition of enzyme or the addition of NADH. The headspace was sampled (0.4 ml) every 3.5 min, and percent hydrogen in the gas phase was determined by a gas chromatograph equipped with a reductive gas analyzer. The concentration of NADH and NADPH was 1 mM. A reduced ferredoxin-generating system was used, consisting of 10 mM pyruvate, 1 mM CoA, 0.1 mM thiamine pyrophosphate, 10 μM clostridial or *S. wolfei* ferredoxin, and 0.1 U of clostridial pyruvate:ferredoxin oxidoreductase.

Assays were set up to determine the final hydrogen concentrations obtained at different NADH/NAD^+ ratios and pH values. The conditions tested included a NADH/NAD^+ ratio of either 1.0 or 1.5 with a total pyridine nucleotide pool size of 5 mM with a buffer of 100 mM potassium phosphate at pH 6.5 or 7.0. The ratios of NADH to NAD^+ used in the above-described experiments were determined from the measured hydrogen partial pressures of growing *S. wolfei* cultures. Final hydrogen concentrations were determined in duplicate from sealed serum bottles after the reaction mixture was incubated for 24 h at room temperature.

It was previously reported that the presence of trace amounts of viologen dyes in cuvettes and stoppers can decouple bifurcating reactions (48). Hydrogen production assays involving NADH were performed using serum bottles and rubber stoppers that were not previously exposed to viologen dyes. Hydrogen-oxidizing assays were performed with stoppers that were not previously exposed to viologen dyes and with extensively washed cuvettes. Methyl viologen reduction assays were done after all other assays were completed.

Analytical techniques. Protein concentration was determined by using the Bradford protein assay (Thermo Fisher Scientific, Waltham, MA) with bovine serum albumin as the standard. SDS-PAGE and native PAGE analyses were performed using precast Novex 8 to 16% Tris-glycine (Life Technologies Co., Carlsbad, CA) according to the manufacturer's instructions. Gels were stained using Coomassie brilliant blue G-250 (Thermo Fisher Scientific, Waltham, MA). Bands from the native gel were excised for peptide identification. The protein in the excised band was digested with trypsin and subjected to high-performance liquid chromatography-tandem mass spectrometry (HPLC-MS/MS) performed by the Laboratory for Molecular Biology and Cytometry Research at OUHSC (Oklahoma City, OK). Resulting peptide fragments were identified by Mascot search and compared to the NCBI nonredundant (nr) database.

Molecular mass of recombinant Hyd1ABC was determined by size exclusion chromatography. Size exclusion chromatography was performed using a Superdex 200 10/300 GL (GE Healthcare Life Sciences) calibrated with gel filtration standards (Bio-Rad Laboratories, Hercules, CA) using a buffer of 50 mM potassium phosphate (pH 7.5) with 0.5 M NaCl at a flow rate of 0.45 ml/min.

Iron content of the purified recombinant Hyd1ABC was determined using a ferrozine assay (49). Identification and quantification of bound flavin were performed by HPLC. The purified recombinant Hyd1ABC was washed 20-fold by ultrafiltration using flavin-free 50 mM Tris-HCl (pH 7.5) and boiled for 10 min, and denatured protein was removed by centrifugation at 13,000 $\times$ *g* for 10 min. The supernatant was then analyzed using a Kromasil 100-10-C_{18} column (250 by 4.6 mm) using a buffer of 25% methanol in 50 mM ammonium formate similar to a previous HPLC technique (50) with a UV detector set to 275 nm. Retention times and peak areas were compared to FAD and FMN standards.

Hydrogen concentration was determined by a gas chromatograph (30, 51) equipped with a reductive gas detector Peak Performer RCP-910 (Peak Laboratories, Mountain View, CA). Hydrogen concentrations were determined by comparing peak areas to standards containing hydrogen concentrations of 0.01 to 1%.

Biochemicals and enzymes. NADH, NAD^+, FMN, FAD, pyruvate, thiamine pyrophosphate, methyl viologen, and coenzyme A were purchased from Sigma-Aldrich (St. Louis, MO). Clostridial ferredoxin (33) and pyruvate ferredoxin oxidoreductase (52) were purified from *Clostridium pasteurianum* (strain DSM 525).

Culture growth conditions. Pure cultures of *S. wolfei* (strain DSM 2245B) and cocultures with *M. hungatei* strain JF-1 (strain ATCC 27890) were grown anaerobically with resazurin as the redox indicator and cysteine sulfide (0.05%) as the reducing agent. The culture medium consisted of 10 ml · $liter^{-1}$ each of mineral, trace metal, and vitamin solutions (53) prepared anaerobically under a N_2/CO_2 (80:20) atmosphere with 3.5 g · $liter^{-1}$ $NaHCO_3$ as the buffering agent and 20 mM butyrate or crotonate as the substrate. Cultures were established in triplicate with 160-ml culture medium and 90-ml headspace volumes and incubated at 37°C with shaking at 80 rpm. Growth was monitored at OD_{600} with measurements for fatty acid, hydrogen, and methane concentrations made at 4-day intervals. Determinations of butyrate, crotonate, and methane concentrations were performed by HPLC and gas chromatography-flame ionization detector (GC-FID) as described previously (9) while hydrogen concentrations were determined as described for hydrogen production assays.

SUPPLEMENTAL MATERIAL

Supplemental material for this article may be found at https://doi.org/10.1128/AEM.01335-17.

SUPPLEMENTAL FILE 1, PDF file, 0.5 MB.

ACKNOWLEDGMENTS

We thank N. Q. Wofford for technical assistance.

The initial cloning was developed and accomplished as part of the Biological and

Electron Transfer and Catalysis (BETCy) EFRC, an Energy Frontier Research Center funded by the U.S. Department of Energy, Office of Science, Basic Energy Sciences under Award DE-SC0012518 to J.W.P. Additional production and characterization of Hyd1ABC were supported by National Science Foundation grant 1515843 to M.J.M. The funders had no role in study design, data collection and interpretation, or the decision to submit the work for publication.

REFERENCES

1. McInerney MJ, Bryant MP, Hespell RB, Costerton JW. 1981. *Syntrophomonas wolfei* gen. nov. sp. nov., an anaerobic, syntrophic, fatty acid-oxidizing bacterium. Appl Environ Microbiol 41:1029–1039.
2. McInerney MJ, Bryant MP. 1981. Basic principles of bioconversions in anaerobic digestion and methanogenesis, p 277–296. *In* Sofer SS, Zaborsky OR (ed), Biomass conversion processes for energy and fuels. Springer US, Boston, MA. https://doi.org/10.1007/978-1-4757-0301-6_15.
3. Schink B. 1997. Energetics of syntrophic cooperation in methanogenic degradation. Microbiol Mol Biol Rev 61:262–280.
4. Sieber JR, Sims DR, Han C, Kim E, Lykidis A, Lapidus AL, McDonnald E, Rohlin L, Culley DE, Gunsalus R, McInerney MJ. 2010. The genome of *Syntrophomonas wolfei*: new insights into syntrophic metabolism and biohydrogen production. Environ Microbiol 12:2289–2301.
5. Schmidt A, Müller N, Schink B, Schleheck D. 2013. A proteomic view at the biochemistry of syntrophic butyrate oxidation in *Syntrophomonas wolfei*. PLoS One 8:e56905. https://doi.org/10.1371/journal.pone.0056905.
6. Wofford NQ, Beaty PS, McInerney MJ. 1986. Preparation of cell-free extracts and the enzymes involved in fatty acid metabolism in *Syntrophomonas wolfei*. J Bacteriol 167:179–185. https://doi.org/10.1128/jb.167.1.179-185.1986.
7. Sieber JR, Crable BR, Sheik CS, Hurst GB, Rohlin L, Gunsalus RP, McInerney MJ. 2015. Proteomic analysis reveals metabolic and regulatory systems involved in the syntrophic and axenic lifestyle of *Syntrophomonas wolfei*. Front Microbiol 6:115. https://doi.org/10.3389/fmicb.2015.00115.
8. Crable BR, Sieber JR, Mao X, Alvarez-Cohen L, Gunsalus R, Ogorzalek Loo RR, Nguyen H, McInerney MJ. 2016. Membrane complexes of *Syntrophomonas wolfei* involved in syntrophic butyrate degradation and hydrogen formation. Front Microbiol 7:1795. https://doi.org/10.3389/fmicb.2016.01795.
9. Sieber JR, Le HM, McInerney MJ. 2014. The importance of hydrogen and formate transfer for syntrophic fatty, aromatic and alicyclic metabolism. Environ Microbiol 16:177–188. https://doi.org/10.1111/1462-2920.12269.
10. Sieber JR, McInerney MJ, Gunsalus RP. 2012. Genomic insights into syntrophy: the paradigm for anaerobic metabolic cooperation. Annu Rev Microbiol 66:429–452. https://doi.org/10.1146/annurev-micro-090110-102844.
11. Schut GJ, Adams MW. 2009. The iron-hydrogenase of *Thermotoga maritima* utilizes ferredoxin and NADH synergistically: a new perspective on anaerobic hydrogen production. J Bacteriol 191:4451–4457. https://doi.org/10.1128/JB.01582-08.
12. Malki S, Saimmaime I, De Luca G, Rousset M, Dermoun Z, Belaich JP. 1995. Characterization of an operon encoding an NADP-reducing hydrogenase in *Desulfovibrio fructosovorans*. J Bacteriol 177:2628–2636. https://doi.org/10.1128/jb.177.10.2628-2636.1995.
13. Hartmann T, Leimkühler S. 2013. The oxygen-tolerant and NAD^+-dependent formate dehydrogenase from *Rhodobacter capsulatus* is able to catalyze the reduction of CO_2 to formate. FEBS J 280:6083–6096. https://doi.org/10.1111/febs.12528.
14. Schuchmann K, Müller V. 2012. A bacterial electron-bifurcating hydrogenase. J Biol Chem 287:31165–31171. https://doi.org/10.1074/jbc.M112.395038.
15. Wang S, Huang H, Kahnt J, Thauer RK. 2013. A reversible electron-bifurcating ferredoxin- and NAD-dependent [FeFe]-hydrogenase (HydABC) in *Moorella thermoacetica*. J Bacteriol 195:1267–1275. https://doi.org/10.1128/JB.02158-12.
16. Zheng Y, Kahnt J, Kwon IH, Mackie RI, Thauer RK. 2014. Hydrogen formation and its regulation in *Ruminococcus albus*: involvement of an electron-bifurcating [FeFe]-hydrogenase, of a non-electron-bifurcating [FeFe]-hydrogenase, and of a putative hydrogen-sensing [FeFe]-hydrogenase. J Bacteriol 196:3840–3852. https://doi.org/10.1128/JB.02070-14.
17. Jackson BE, McInerney MJ. 2002. Anaerobic microbial metabolism can proceed close to thermodynamic limits. Nature 415:454–456. https://doi.org/10.1038/415454a.
18. Girbal L, von Abendroth G, Winkler M, Benton PM, Meynial-Salles I, Croux C, Peters JW, Happe T, Soucaille P. 2005. Homologous and heterologous overexpression in *Clostridium acetobutylicum* and characterization of purified clostridial and algal Fe-only hydrogenases with high specific activities. Appl Environ Microbiol 71:2777–2781. https://doi.org/10.1128/AEM.71.5.2777-2781.2005.
19. King PW, Posewitz MC, Ghirardi ML, Seibert M. 2006. Functional studies of [FeFe] hydrogenase maturation in an *Escherichia coli* biosynthetic system. J Bacteriol 188:2163–2172. https://doi.org/10.1128/JB.188.6.2163-2172.2006.
20. Amos DA, McInerney MJ. 1989. Poly-β-hydroxyalkanoate in *Syntrophomonas wolfei*. Arch Microbiol 152:172–177. https://doi.org/10.1007/BF00456097.
21. McInerney MJ, Bryant MP, Pfennig N. 1979. Anaerobic bacterium that degrades fatty acids in syntrophic association with methanogens. Arch Microbiol 122:129–135. https://doi.org/10.1007/BF00411351.
22. Poudel S, Tokmina-Lukaszewska M, Colman DR, Refai M, Schut GJ, King PW, Maness PC, Adams MW, Peters JW, Bothner B, Boyd ES. 2016. Unification of [FeFe]-hydrogenases into three structural and functional groups. Biochim Biophys Acta 1860:1910–1921. https://doi.org/10.1016/j.bbagen.2016.05.034.
23. Schuchmann K, Müller V. 2014. Autotrophy at the thermodynamic limit of life: a model for energy conservation in acetogenic bacteria. Nat Rev Microbiol 12:809–821. https://doi.org/10.1038/nrmicro3365.
24. Wimpenny JWT, Firth A. 1972. Levels of nicotinamide adenine dinucleotide and reduced nicotinamide adenine dinucleotide in facultative bacteria and the effect of oxygen. J Bacteriol 111:24–32.
25. de Graef MR, Alexeeva S, Snoep JL, Teixeira de Mattos MJ. 1999. The steady-state internal redox state (NADH/NAD) reflects the external redox state and is correlated with catabolic adaptation in *Escherichia coli*. J Bacteriol 181:2351–2357.
26. Snoep JL, Joost M, de Mattos T, Neijssel OM. 1991. Effect of the energy source on the NADH/NAD ratio and on pyruvate catabolism in anaerobic chemostat cultures of *Enterococcus faecalis* NCTC 775. FEMS Microbiol Lett 81:63–66. https://doi.org/10.1111/j.1574-6968.1991.tb04713.x.
27. Wallrabenstein C, Schink B. 1994. Evidence of reversed electron transport in syntrophic butyrate or benzoate oxidation by *Syntrophomonas wolfei* and *Syntrophus buswellii*. Arch Microbiol 162:136–142. https://doi.org/10.1007/BF00264387.
28. Boone DR, Johnson RL, Liu Y. 1989. Diffusion of the interspecies electron carriers H_2 and formate in methanogenic ecosystems and its implications in the measurement of K_m for H_2 or formate uptake. Appl Environ Microbiol 55:1735–1741.
29. Conrad R, Schink B, Phelps TJ. 1986. Thermodynamics of H_2-consuming and H_2-producing metabolic reactions in diverse methanogenic environments under in situ conditions. FEMS Microbiol Lett 38:353–360. https://doi.org/10.1111/j.1574-6968.1986.tb01748.x.
30. Montag D, Schink B. 2016. Biogas process parameters–energetics and kinetics of secondary fermentations in methanogenic biomass degradation. Appl Microbiol Biotechnol 100:1019–1026. https://doi.org/10.1007/s00253-015-7069-0.
31. Schmidt O, Hink L, Horn MA, Drake HL. 2016. Peat: home to novel syntrophic species that feed acetate- and hydrogen-scavenging methanogens. ISME J 10:1954–1966. https://doi.org/10.1038/ismej.2015.256.
32. Aono S, Bryant FO, Adams MW. 1989. A novel and remarkably thermostable ferredoxin from the hyperthermophilic archaebacterium *Pyrococ-*

cus furiosus. J Bacteriol 171:3433–3439. https://doi.org/10.1128/jb.171.6.3433-3439.1989.
33. Schönheit P, Wäscher C, Thauer RK. 1978. A rapid procedure for the purification of ferredoxin from clostridia using polyethyleneimine. FEBS Lett 89:219–222. https://doi.org/10.1016/0014-5793(78)80221-X.
34. Beaty PS, McInerney MJ. 1987. Growth of *Syntrophomonas wolfei* in pure culture on crotonate. Arch Microbiol 147:389–393. https://doi.org/10.1007/BF00406138.
35. Marchler-Bauer A, Derbyshire MK, Gonzales NR, Lu S, Chitsaz F, Geer LY, Geer RC, He J, Gwadz M, Hurwitz DI, Lanczycki CJ, Lu F, Marchler GH, Song JS, Thanki N, Wang Z, Yamashita RA, Zhang D, Zheng C, Bryant SH. 2015. CDD: NCBI's conserved domain database. Nucleic Acids Res 43:D222–D226. https://doi.org/10.1093/nar/gku1221.
36. Wang S, Huang H, Kahnt J, Thauer RK. 2013. *Clostridium acidurici* electron-bifurcating formate dehydrogenase. Appl Environ Microbiol 79:6176–6179. https://doi.org/10.1128/AEM.02015-13.
37. Soboh B, Linder D, Hedderich R. 2004. A multisubunit membrane-bound [NiFe] hydrogenase and an NADH-dependent Fe-only hydrogenase in the fermenting bacterium *Thermoanaerobacter tengcongensis*. Microbiology 150:2451–2463. https://doi.org/10.1099/mic.0.27159-0.
38. Chowdhury NP, Mowafy AM, Demmer JK, Upadhyay V, Koelzer S, Jayamani E, Kahnt J, Hornung M, Demmer U, Ermler U, Buckel W. 2014. Studies on the mechanism of electron bifurcation catalyzed by electron transferring flavoprotein (Etf) and butyryl-CoA dehydrogenase (Bcd) of *Acidaminococcus fermentans*. J Biol Chem 289:5145–5157. https://doi.org/10.1074/jbc.M113.521013.
39. Lubner CE, Jennings DP, Mulder DW, Schut GJ, Zadvornyy OA, Hoben JP, Tokmina-Lukaszewska M, Berry L, Nguyen DM, Lipscomb GL, Bothner B, Jones AK, Miller AF, King PW, Adams MWW, Peters JW. 2017. Mechanistic insights into energy conservation by flavin-based electron bifurcation. Nat Chem Biol 13:655–659. https://doi.org/10.1038/nchembio.2348.
40. Sousa DZ, Smidt H, Alves MM, Stams AJM. 2007. *Syntrophomonas zehnderi* sp. nov., an anaerobe that degrades long-chain fatty acids in co-culture with *Methanobacterium formicicum*. Int J Syst Evol Microbiol 57:609–615. https://doi.org/10.1099/ijs.0.64734-0.
41. Sekiguchi Y, Kamagata Y, Nakamura K, Ohashi A, Harada H. 2000. *Syntrophothermus lipocalidus* gen. nov., sp. nov., a novel thermophilic, syntrophic, fatty-acid-oxidizing anaerobe which utilizes isobutyrate. Int J Syst Evol Microbiol 50:771–779. https://doi.org/10.1099/00207713-50-2-771.
42. Svetlitshnyi V, Rainey F, Wiegel J. 1996. *Thermosyntropha lipolytica* gen. nov., sp. nov., a lipolytic, anaerobic, alkalitolerant, thermophilic bacterium utilizing short- and long-chain fatty acids in syntrophic coculture with a methanogenic archaeum. Int J Syst Evol Microbiol 46:1131–1137.
43. Worm P, Koehorst JJ, Visser M, Sedano-Núñez VT, Schaap PJ, Plugge CM, Sousa DZ, Stams AJM. 2014. A genomic view on syntrophic versus non-syntrophic lifestyle in anaerobic fatty acid degrading communities. Biochim Biophys Acta Bioenergetics 1837:2004–2016. https://doi.org/10.1016/j.bbabio.2014.06.005.
44. Kung JW, Seifert J, von Bergen M, Boll M. 2013. Cyclohexane carboxyl-coenzyme A (CoA) and cyclohex-1-ene-1-carboxyl-CoA dehydrogenases, two enzymes involved in the fermentation of benzoate and crotonate in *Syntrophus aciditrophicus*. J Bacteriol 195:3193–3200. https://doi.org/10.1128/JB.00322-13.
45. Meyer B, Kuehl J, Deutschbauer AM, Price MN, Arkin AP, Stahl DA. 2013. Variation among *Desulfovibrio* species in electron transfer systems used for syntrophic growth. J Bacteriol 195:990–1004. https://doi.org/10.1128/JB.01959-12.
46. Schmidt A, Frensch M, Schleheck D, Schink B, Müller N. 2014. Degradation of acetaldehyde and its precursors by *Pelobacter carbinolicus* and *P. acetylenicus*. PLoS One 9:e115902. https://doi.org/10.1371/journal.pone.0115902.
47. Müller N, Schleheck D, Schink B. 2009. Involvement of NADH:acceptor oxidoreductase and butyryl coenzyme A dehydrogenase in reversed electron transport during syntrophic butyrate oxidation by *Syntrophomonas wolfei*. J Bacteriol 191:6167–6177. https://doi.org/10.1128/JB.01605-08.
48. Kaster AK, Moll J, Parey K, Thauer RK. 2011. Coupling of ferredoxin and heterodisulfide reduction via electron bifurcation in hydrogenotrophic methanogenic archaea. Proc Natl Acad Sci U S A 108:2981–2986. https://doi.org/10.1073/pnas.1016761108.
49. Riemer J, Hoepken HH, Czerwinska H, Robinson SR, Dringen R. 2004. Colorimetric ferrozine-based assay for the quantitation of iron in cultured cells. Anal Biochem 331:370–375. https://doi.org/10.1016/j.ab.2004.03.049.
50. Seedorf H, Dreisbach A, Hedderich R, Shima S, Thauer RK. 2004. $F_{420}H_2$ oxidase (FprA) from *Methanobrevibacter arboriphilus*, a coenzyme F_{420}-dependent enzyme involved in O_2 detoxification. Arch Microbiol 182:126–137. https://doi.org/10.1007/s00203-004-0675-3.
51. Seiler W, Giehl H, Roggendorf P. 1980. Detection of carbon monoxide and hydrogen by conversion of mercury oxide to mercury vapor. Atmos Technol 12:40–45.
52. Wahl RC, Orme-Johnson WH. 1987. Clostridial pyruvate oxidoreductase and the pyruvate-oxidizing enzyme specific to nitrogen fixation in *Klebsiella pneumoniae* are similar enzymes. J Biol Chem 262:10489–10496.
53. Tanner RS. 2007. Cultivation of bacteria and fungi, p 69–78. *In* Hurst CJ, Crawford RL, Garland JL, Lipson DA, Mills AL, Stetzenbach LD (ed), Manual of environmental microbiology, 3rd ed. American Society for Microbiology, Washington, DC. https://doi.org/10.1128/9781555815882.ch6.